



Low-concentration salting of cod loins

The effect on biochemical properties and predicted water retention during heating

Jordbrekk Blikra, Marthe ; Jessen, Flemming; Feyissa, Aberham Hailu; Vaka, Mette R.; Skipnes, Dagbjørn

Published in:
LWT

Link to article, DOI:
[10.1016/j.lwt.2019.108702](https://doi.org/10.1016/j.lwt.2019.108702)

Publication date:
2020

Document Version
Peer reviewed version

[Link back to DTU Orbit](#)

Citation (APA):

Jordbrekk Blikra, M., Jessen, F., Feyissa, A. H., Vaka, M. R., & Skipnes, D. (2020). Low-concentration salting of cod loins: The effect on biochemical properties and predicted water retention during heating. *LWT*, 118, Article 108702. <https://doi.org/10.1016/j.lwt.2019.108702>

General rights

Copyright and moral rights for the publications made accessible in the public portal are retained by the authors and/or other copyright owners and it is a condition of accessing publications that users recognise and abide by the legal requirements associated with these rights.

- Users may download and print one copy of any publication from the public portal for the purpose of private study or research.
- You may not further distribute the material or use it for any profit-making activity or commercial gain
- You may freely distribute the URL identifying the publication in the public portal

If you believe that this document breaches copyright please contact us providing details, and we will remove access to the work immediately and investigate your claim.

1 Low-concentration salting of cod loins: The effect on biochemical properties and predicted water
2 retention during heating

3 Marthe J. Blikra^{1, 2*}, Flemming Jessen², Aberham H. Feyissa², Mette R. Vaka³, Dagbjørn Skipnes¹

4 1. Nofima, Norwegian Institute of Food, Fisheries and Aquaculture Research, Norway

5 2. DTU Food Production Engineering, Denmark

6 3. University of Stavanger, Faculty of Science and Technology, Norway

7 Corresponding author. E-mail: marthe.blikra@nofima.no

8 Abstract

9 Low levels of salt are frequently used to increase flavor and water retention in cod. This alters the
10 biochemical properties of cod during heating. In this paper, properties needed to mathematically
11 model moisture transfer during cooking – water holding capacity and storage modulus – were
12 determined for cod containing 0.06, 1 and 3 g/100 g NaCl. Protein denaturation and microstructure
13 was also investigated to increase the understanding of quality effects of salt during cooking. A model
14 was established to investigate the effect of the measured storage modulus and water holding
15 capacity on the predicted moisture retention during heating. Salting lead to a higher water holding
16 capacity, less hardening of the muscle tissue during heating, diffused protein denaturation peaks and
17 caused swelling of the muscle fibers. By interchanging the acquired variables in the model of coupled
18 heat and moisture transfer, we found a higher predicted water retention during cooking of brined
19 cod compared to unsalted cod. This knowledge may be utilized in creating modeling tools for
20 optimization of cooking processes, which may support chefs and ready-to-eat meal producers in
21 reducing weight loss and improving the texture and juiciness of their products.

22 1. Introduction

23 Mathematical modeling is a powerful tool which may be used in the food industry, catering and
24 restaurants for creating cooking protocols tailored to the specific fish product at hand. Using physics-
25 based mathematical modeling, it is possible to try out endless combinations of convection oven input
26 parameters – such as temperature, relative humidity and heating time – and observe effects on
27 quality parameters which may be included in the model as output. Such quality parameters may
28 include texture – especially hardness or toughness; water holding capacity – which is related to
29 juiciness; and color development (Kong, Tang, Rasco & Crapo, 2007; Ovissipour, Rasco, Tang &
30 Sablani, 2017; Rabeler & Feyissa, 2018a). Moreover, such models can be combined with bacterial
31 inactivation kinetics and kinetics of vitamin breakdown, and this offers opportunities for creating
32 products which are both safe, healthy and tasty.

33 For modeling the moisture transfer during heating, it is commonly assumed that the muscle structure
34 functions like a porous media, for which Darcy's law can be applied (Datta, 2007). Using this
35 approach, properties describing both the muscle structure, the liquid being transported, and their
36 interactions are needed. The driving force in Darcy's law has been hypothesized to be the swelling
37 pressure that originates when proteins denature and muscle foods swell or shrink, which can be
38 determined from the water holding capacity and storage modulus of a product (Barrière & Leibler,
39 2003; van der Sman, 2007). These properties have been determined for meat, chicken and cod, and
40 the porous media approach has been used for modeling moisture transfer during heating of these
41 foods (eg. Feyissa, Gernaey & Adler-Nissen, 2013; Rabeler & Feyissa, 2018b; Blikra, Skipnes & Feyissa,
42 2019). However, the properties of the muscle, especially the water holding capacity – which
43 describes the ability of a food to hold on to water when a pressure is applied – may change
44 drastically when salt is added. Salt is commonly applied to cod before heating, and thus it is
45 important to know the extent of which water holding capacity and storage modulus are affected by
46 salt concentration during heating.

47 Addition of low concentrations of salt (< 5.8 g/100 g NaCl) increase the ability of muscle foods to hold
48 on to water, which decrease the amount of liquid exudated during storage of raw fish (Larsen &
49 Elvevoll, 2008; Larsen, Olsen, Kristoffersen & Elvevoll, 2008) and during heating (Kong, Oliveira, Tang,
50 Rasco & Crapo, 2008; Ofstad, Kidman, Myklebust, Olsen & Hermansson, 1996). The increased
51 retention of moisture is caused by a displacement in the isoelectric point, changing the pH at which
52 the muscle proteins bind water more effectively. In addition to being dependent on the salt
53 concentration (Johnsen, Jørgensen, Birkeland, Skipnes & Skåra, 2009), the water holding capacity of
54 fish show changes corresponding to the denaturation of major protein groups (Skipnes, Johnsen,
55 Skåra, Sivertsvik & Lekang, 2011).

56 The other property needed to determine the swelling pressure during cooking, namely the storage
57 modulus, is a rheological property which is correlated with the textural property of hardness. The
58 storage modulus of extracted fish proteins and surimi pastes have been well documented. However,
59 since the effect of salt on rheological properties depend on processing conditions and addition of
60 other additives (eg. Cheow, Yu, & Howell, 1999; Kobayashi & Park, 2017), these results cannot be
61 adopted directly to processing of lightly salted fish muscle. On the other hand, the hardness of brined
62 fish muscle has been assessed using more traditional methods. Sensory analysis was used to assess
63 the hardness of cod brined for 10 min in 5 g/100 g NaCl followed by heating at 95 °C for 10 min in a
64 water bath (Esaiassen *et al.*, 2004). The result indicated an increased softness of brined cod
65 compared to unsalted samples. This correlates with measurements of the force required to pull
66 bones from cod muscle, which decreased with increasing salt concentration in the brine from 1.5-6
67 g/100 g NaCl (Larsen *et al.*, 2008). As measured using a compression test, salmon brined in 1.5 g/100
68 g NaCl also showed a lower shear force after heating at 121.1 °C for 10-60 min compared to unsalted
69 salmon (Kong *et al.*, 2008).

70 It is appropriate to mention that even though salting of fish, especially cod, is an ancient tradition, it
71 is important to consider all foods in a more general perspective of food health. There is strong
72 evidence that high levels of salt in the diet may cause unfavorable medical conditions, especially

73 raised blood pressure and in turn cardiovascular disease (He & MacGregor, 2009), and claims to
74 reduce the amount of salt in processed foods have thus been raised (Asaria, Chisholm, Mathers,
75 Ezzati & Beaglehole, 2007). In addition to demanding less salt, consumers also demand “natural
76 foods” without artificial preservatives including phosphates which are commonly used to increase
77 water retention in muscle foods (Beath, Cousin & Siegrist, 2014; Evans, de Challemaison & Cox,
78 2010; Zink, 1997). It is important to offer consumers a choice to eat preservative-free food, however
79 for the consumers who prefer fish products which are higher in flavor and juiciness, an option where
80 a sufficiently low level of salt is used so that it does not cause damage to public health may be
81 provided. It is our belief that complex modeling could be used to find this level. For restaurants,
82 catering, and the ready-meal industry, adjusting the sodium content in the rest of the meal, for
83 instance by serving cod with vegetables and low-sodium sauce, is also a suitable option.

84 The objective of this paper was 1) to investigate the changes in important moisture transfer
85 properties for cod brined at low concentrations of salt, 2) to increase the understanding of the
86 quality effects of salt on cod during cooking, and finally 3) to enable optimization of convection oven
87 cooking of lightly salted cod through mathematical modeling.

88 2. Materials and methods

89 2.1. Raw material

90 Farmed Atlantic cod (*Gadus morhua*) weighing 2-4 kg were starved for 9 d, killed by a blow to the
91 head, bled in seawater for 25 min, filleted (pre-rigor), and transported on ice to our lab (December
92 2017). The fillets were stored at 0-2 °C (5 d) to undergo *rigor mortis*, after which they were cut into
93 pieces of 100-150 g. Untreated samples were quick-frozen in a blast freezer (<15 min) at -60 °C,
94 vacuum packed at 7.66 kPa to avoid thawing, and stored at -80 °C until analysis to maintain freshness
95 and avoid major changes in water state (Burgaard & Jørgensen, 2010). The remaining samples were
96 brined in individual bags with 2 L brine (0, 1.5 and 4.5 g/100 g NaCl) per fish piece, for 48 h at 0-2 °C,
97 lightly patted dry with a paper towel, followed by processing and storage as described for untreated
98 samples. A flow chart summarizing the processing steps is given in Figure 1.

99 2.2. Characterization of raw material

100 Ten specimens were removed from the slaughter-line one at a time before bleeding. Their initial
101 muscle pH and blood lactate was measured. Fish length (L ; m), as well as mass of whole fish and liver
102 (W , LW ; kg) were used to calculate the hepatosomatic index ($HSI = \frac{LW}{W} * 100$) and condition factor
103 ($K = \frac{W}{L^3} * 100$).

104 The weight gain during brining was analyzed by weighing 10 loins prior to and after brining, after
105 lightly patting dry with a paper towel. Analysis of total aerobic count was performed according to
106 NMKL 184 (2006) on raw material after processing and freezing (n=3). Final pH after processing and
107 freezing was measured in a 1:1 solution of sample and 0.1 mol/L KCl (10-40 g each), using a Mettler
108 Toledo Five Easy Plus pH meter (FEP20, Zürich, Switzerland) with an LE438 electrode. The
109 measurement was performed in duplicate on four samples from different specimen.

110 2.3. Sample preparation

111 The temperature of frozen loins was gradually raised by following the steps shown in Figure 1, to
112 allow cutting the cod pieces into samples of appropriate size. For analysis of water holding capacity

113 (WHC), salt and pH, frozen pieces of cod were cut horizontally into 3 mm thick slices using a meat
114 slicer. For rheology, disks of 30 mm were cut from the muscle slices using a heavy duty round hollow
115 punch – a hand-held device with a sharp-edged pipe attached to a handle. Any brown muscle and
116 uneven areas were avoided during cutting. The white fish muscle surrounding the disks was finely
117 chopped for DSC analysis. To avoid thawing of the samples, the preparation was performed in a chill
118 room with circulating air at 0-2 °C, followed by vacuum-packing in appropriately sized polyethylene
119 bags at a pressure which had previously shown not to thaw the samples (7.66 kPa). The samples
120 were then put back for storage at -80 °C until analysis (<6 mo).

121 2.4. Salt concentration

122 The salt concentration after processing and freezing was measured as total chloride content by
123 titration with silver chloride (Mettler Toledo T7), according to ISO 5943 IDF 88 with some deviations.
124 1.5 g homogenized sample was mixed with 50 mL distilled water at 55 °C for 1 h without subsequent
125 blending. Two samples from the surface and core positions of four loins were analyzed for each
126 parameter (n=2x4), except untreated cod which was analyzed without regard to position (n=8). Going
127 forward, the salted samples (brined at 1.5 and 4.5 g/100g NaCl) are referred to using the average
128 measured concentration of salt, 1 and 3 g/100 g NaCl, respectively (Table 1). The samples brined in
129 pure water are referred to as “water-brined” samples, and the group “unsalted samples” include
130 both water-brined and untreated samples.

131 2.5. Differential scanning calorimetry

132 Heat denaturation was analyzed using a Mettler Toledo DSC1 and a modified version of the
133 methodology described by Skipnes, Van der Plancken, Van Loey & Hendrickx (2008). Samples of
134 51.4 ± 6.5 mg were weighed into stainless steel crucibles (Mettler Toledo medium pressure \varnothing 7 mm
135 with pin), sealed with a Viton O-ring and analyzed at a rate of 2.5 K/min from 2-100 °C. Deionized
136 water corresponding to the amount of water in the sample (40 mg) was used in the reference pan to
137 remove the noise of water from the resulting thermograms. Raw samples (n=6-8) and samples

138 isothermally heated in a GR150 water bath (10 min; n=2) at either 25, 30, 35, 40, 45, 55, 60, or 65 °C
139 were used, except water-brined samples which were not heated at 30 °C. The heated samples were
140 cooled in ice water (> 30 s) prior to DSC analysis. The thermograms were analyzed using the software
141 StarE version 14.00 (Mettler Toledo). A spline baseline was used for analysis of all peaks. Data was
142 reported as peak denaturation temperature (PDT) and normalized (residual) denaturation enthalpy
143 (h_{den}) of each detected peak.

144 2.6. Water holding capacity

145 Water holding capacity (WHC) was analyzed as described by Skipnes, Østby & Hendrickx (2007), with
146 some alterations. Briefly, 5.12 ± 0.02 g of fish pieces were gently ripped to appropriate size and
147 weighed into cooled, pre-weighed steel sample cups of height 37 and $\varnothing 36$ mm (Skipnes *et al.*, 2007).
148 The cups had an adjustable, central filter, allowing the fish sample to be rotated up until it touched
149 the lid of the cup, and the expelled liquid was allowed to exit through the filter to the removable
150 bottom. For analysis of cooked samples, the filled sample cup was isothermally heated in a water
151 bath (GR150, Grant Instruments, Cambridge, UK). Each cup was heated at either 25, 30, 35, 40, 45,
152 55, 60, 65, 70 or 100 °C, before cooling in ice water for 5 min. The cups were kept cold until removal
153 of the cook loss using paper towels, followed by centrifugation (Rotina 420R, Hettich, Tuttlingen,
154 Germany) at 4 °C for 15 min at 528 g (Skipnes *et al.*, 2007; Skipnes *et al.*, 2011). WHC was determined
155 as the remaining mass after centrifugation as a fraction of the original, raw mass and as g hold water
156 /g dry weight (n=8). The gravimetrically determined (18 h, 105 °C) water content of representative
157 samples (n=8) of each salt concentration was used in the calculation (Table 1).

158 2.7. Rheology

159 Rheological measurements were performed using a DHR-2 (TA Instruments, New Castle, DE, USA)
160 with a 20 mm cross-hatched parallel plate and temperature control connected to a heat exchanger
161 (P/N 953260.901 TGA), as described by Blikra *et al.* (2019). Samples were collected one-at-a-time
162 from storage at -80 °C (n=10), thawed in ice water and put on the 0 °C Peltier plate. Temperature

163 ramps were performed at 1.0 Hz, from 0-100 °C, with a heating rate of 2.5 K/min, and with an initial
164 axial force of 0.25 ± 0.1 N. The strain % to be used for the tests were determined from amplitude
165 sweeps performed at a minimum of three temperatures, to ensure testing in a linear viscoelastic
166 region. The strain % determined were 0.05, 0.025, and 0.25 % for water-brined samples and samples
167 containing 1 and 3 g/100 g NaCl, respectively. A solvent trap was placed around the sample and
168 geometry to prevent heat loss and drying, and aluminum foil was placed around the solvent trap for
169 additional prevention of heat loss.

170 2.8. Microstructure

171 Cross-sectional microstructure was analyzed using myotomes separated from muscle samples. In
172 order to dissolve the collagen holding the sheets together and enable separation of the sheets, cubes
173 of approximately 30 mm were vacuum packed (7.66 kPa) in polyethylene bags and heated for 20 min
174 at 30 °C in a GR150 water bath. The samples were subsequently frozen in liquid nitrogen and stored
175 at -80 °C until analysis (unsalted <13 mo; brined < 3 mo; Figure 1). Upon analysis, frozen samples
176 were embedded in tissue freezing medium (Leica, 14020108926, Wetzlar, Germany), and cut into 10
177 μm slices at -20 °C using a Leica CM1860 UV cryostat. The slices were transferred to microscopy
178 slides and stained with Orange G and Methyl blue (Sigma-Aldrich, St. Louis, MO, USA), followed by
179 inspection using a Leica MZ8 stereo microscope (San Jose, CA, USA). Images were prepared with an
180 integrated camera above the lens (VisiCam 10.0, VWR®, Leuven, Belgium). ImageJ (Version 1.52b, Fiji)
181 was used for calibration of pixel size. For each sample group, the analysis was conducted in triplicate.

182 2.9. Model prediction

183 A mathematical model was established to investigate the effect of the measured difference in WHC
184 and storage modulus on the predicted mass loss. A similar model was previously published (Blikra *et*
185 *al.*, 2019), but for convenience, a summary of the model is given below.

186 2.9.1. Governing equations

187 2.9.1.1. Heat transfer

188 The heat transfer is described by Eq. 1:

189
$$\rho c_p \left(\frac{\partial T}{\partial t} \right) + \nabla \cdot (-k \nabla T) + \rho_w c_{p,w} \mathbf{u}_w \cdot \nabla T = 0 \quad (1)$$

190 where ρ , c_p , and k – the density (1060 kg/m³), specific heat (3650 J/(kg K)) and thermal conductivity
191 (0.515 W/(m K)) – are the material properties of the fish which are obtained from Skipnes *et al.*
192 (2007). The thermophysical properties (density, ρ_w (986 kg/m³) and specific heat, $c_{p,w}$ (4190 J/(kg K))
193 of the liquid transported were approximated from the properties of water at 55 °C (Singh &
194 Heldman, 2014). ∇ is the three-dimensional del operator, i.e. partial derivative in x, y, and z direction
195 ($\nabla = \partial / \partial x + \partial / \partial y + \partial / \partial z$). \mathbf{u}_w is the flow velocity of the liquid (m/s) given by Eq. 3, and T is the
196 temperature (K).

197 2.9.1.2. Mass transfer

198 Moisture transfer within the fish sample is based on the conservation of mass (Bird, Stewart, &
199 Lightfoot, 2002), and given by Eq. 2:

200
$$\frac{\partial c}{\partial t} + \nabla \cdot (-D_w \nabla c + \mathbf{u}_w c) = 0 \quad (2)$$

201 where c is the moisture concentration (mol/m³) and D_w is the moisture diffusion coefficient
202 (4×10^{-10} m²/s; Valle & Nickerson, 1968) in the sample. Using a porous media approach (see
203 Section 1), the velocity of the water inside the fish sample, \mathbf{u}_w , was described by Darcy's law (Eq. 3):

204
$$\mathbf{u}_w = -\frac{\kappa G'}{\mu_w} \nabla (C - C_{eq}) \quad (3)$$

205 where κ is the permeability of cod (10^{-17} m²; Datta, 2006), G' is the storage modulus (Eq. 9), and μ_w
206 is the dynamic viscosity of water (Pa s; Singh and Heldman, 2014), given by Eq. 4. C is the mass
207 fraction of water (kg/kg sample), and C_{eq} is the water holding capacity (Eq. 8).

208
$$\mu_w = 2.414 \times 10^{-5} \times 10^{\frac{247.8}{T+133.15}} \quad (4)$$

209 2.9.2. Boundary conditions

210 2.9.2.1. Heat transfer

211 Convective boundary conditions were applied to all external surfaces of the fish sample (eg. Feyissa
212 *et al.*, 2013):

$$213 \quad \mathbf{n} \cdot (-k\nabla T) = (1 - f_h)(h(T_{oven} - T_s)) \quad (5)$$

214 where h is the convective heat transfer coefficient (55 W/(m² K)) and T_{oven} is the temperature of the
215 oven (146.8 °C). f_h is a step function turning the heat transfer off when the surface temperature
216 approaches 100 °C (see Feyissa *et al.*, 2013).

217 2.9.2.2. Mass transfer

218 The mass transfer boundary condition at the fish sample was applied to all external surfaces, except
219 the bottom surface where a no flux condition was assumed. The evaporative flux was modeled using
220 Eq. 6 (Feyissa *et al.*, 2013; Blikra *et al.*, 2019):

$$221 \quad \mathbf{n} \cdot (-D_w \nabla c) = -f_{evap} \frac{h(T_{oven} - T_s)}{H_{evap}} \frac{C_s - C_{air}}{M_w} \quad (6)$$

222 where f_{evap} is the measured fraction of the internal energy used for evaporation, given by Eq. 7
223 (Blikra *et al.*, 2019), H_{evap} is the latent heat of evaporation (2.3×10^6 J/kg), and M_w is the molecular
224 weight of water (18.02 g/mol). C_s is the mass fraction of water at the surface of the sample, and C_{air} is
225 the relative humidity (0.1[-]).

$$226 \quad f_{evap}(T) = 1 + \frac{-f_{max}}{1 + \exp\left(\frac{T - 226.2}{15}\right)} \quad (7)$$

227 2.9.3. Model solution

228 The mathematical model was solved in COMSOL Multiphysics® version 5.4 using the Finite Element
229 Method (FEM). The fish piece was modeled as a rectangle of 20x30x15mm. The geometry was
230 meshed using a free tetrahedral distribution to increase the resolution along the edges of the fish,
231 while the predefined “finer” setting was used for the remaining geometry (Blikra *et al.*, 2019).

232 In the computation, we took advantage of the geometrical symmetry to reduce the computational
233 burden to 1/4th of the required calculations. Thus, along the internal boundaries of the sample,
234 symmetry boundary conditions were assigned to obtain a solution for each element in the full
235 geometry (see Blikra *et al.*, 2019).

236 2.10. Statistical analysis

237 Statistical analysis was performed using Minitab® 18.1. One-way ANOVA with 95 % confidence
238 interval and Tukey post-hoc test was performed for analysis of significant difference. For rheological
239 analysis, measurements every 0.4 °C were collected. To simplify the statistical analysis,
240 measurements every 5 °C were selected for analysis of variance.

241 3. Results and discussion

242 3.1. Characterization of raw material

243 The stress level experienced by the fish during the slaughter process was assessed using initial
244 muscle pH and blood lactate, measured to 7.3 ± 0.1 and 2.5 ± 0.7 mmol/L, respectively, indicating low
245 stress levels. Hepatosomatic index and condition (K) factor were used to assess the nutritional status
246 of the fish. As found by Lambert & Dutil (1997), K-factor and HSI are indicators of muscle and liver
247 energy in cod, respectively. The K-factor was found to be 1.35 ± 0.1 kg/m³, which is comparable to
248 other values reported for farmed cod (Hultmann, Tobiassen, Aas-Hansen, Phu & Rustad, 2016;
249 Kristoffersen *et al.*, 2006a; Kristoffersen, Vang, Larsen & Olsen, 2007). The HSI was found to be
250 14.7 ± 1.3 [–], which indicates good nutritional status, and is slightly higher than other values
251 reported for farmed cod (Kristoffersen *et al.*, 2006a; Kristoffersen, Tobiassen, Steinsund & Olsen,
252 2006b; Kristoffersen *et al.*, 2007).

253 During the brining process all samples absorbed weight, including samples brined in pure water. The
254 amount of uptake increased with increasing salt concentration in the brine from 0 to 4.5 g/100 g
255 (Table 1). No significant difference was found between the microbial load of samples undergoing the

256 different treatments. The total aerobic count averaged 2.3 ± 0.3 cfu/g, indicating good microbial
257 quality.

258 3.2. Differential scanning calorimetry

259 Differential scanning calorimetry (DSC) of untreated samples generally revealed three peaks (Figure
260 2). The peak maximum temperature found for the peaks of untreated cod in this work were in the
261 same range of what was found for farmed, unsalted cod (Skipnes *et al.*, 2008) and wild fresh cod
262 (Hastings, Rodger, Park, Matthews & Anderson, 1985). However, due to differences of the
263 instrument and setup, three peaks were identified instead of five and eight which were found in the
264 other studies. Based on the aforementioned work, peak 1 was attributed to myosin and residual
265 collagen, and peak 2 to sarcoplasmic proteins. Within peak 3 it was often possible to identify two
266 overlapping peaks: the smaller and of lower temperature was attributed to sarcoplasmic proteins,
267 and the larger to actin. In this study, these were analyzed as one peak, with peak denaturation
268 temperature corresponding to actin. It is a logical assumption that the majority of denaturation
269 enthalpy (h_{den}) of this peak comes from denaturation of actin, since the proportion of actin in cod
270 muscle greatly surpasses that of sarcoplasmic proteins. Furthermore, the peak denaturation
271 temperature (PDT) and h_{den} for actin is known from literature (eg. Skipnes *et al.*, 2008) to be in the
272 same range as peak 3 in the present study and does not correspond with observations of
273 sarcoplasmic proteins.

274 For samples that had not been heat-treated before the DSC analysis, the average PDT of myosin
275 (peak 1) was found at 35.8-46.2 °C, with higher values for unsalted specimen (Figure 3). Water-
276 brining shifted the myosin PDT significantly by 3.0 °C on average, from 43.2 for untreated samples to
277 46.2 °C. Salted samples showed a significantly lower myosin PDT and h_{den} compared to unsalted
278 samples. The peak attributed to sarcoplasmic proteins was detected at average temperatures from
279 56.6-58.2 °C, with no significant differences between the sample groups. The exception was samples
280 containing 3 g/100 g NaCl, for which no peak was observed. The average PDT of actin (peak 3)
281 decreased with increasing salt concentration, from 76.1 °C for untreated samples to 66.2 °C for

282 samples containing 3 g/100 g NaCl. The denaturation enthalpy followed the same trend of decreasing
283 absolute value with increasing salt concentration, as was also reported for cod containing higher
284 concentrations of salt (7-20 g/100 g; Thorarinsdottir, Arason, Geirsdottir, Bogason & Kristbergsson,
285 2002).

286 When the samples were heated from 25-65 °C prior to DSC analysis, the residual denaturation
287 enthalpy (h_{den}) and PDT shifted (Figure 3). For all sample groups, the h_{den} of myosin did not change
288 compared to raw samples after heating at 25 °C. For the salted samples, h_{den} of myosin was
289 significantly smaller than for the unsalted samples, and the peak attributed to myosin disappeared
290 after heating at 30-35 °C. Sarcoplasmic proteins (peak 2) were completely denatured after heating at
291 55 °C or above for unsalted samples, and 50 °C or above for samples containing 1 g/100 g NaCl. After
292 heating the samples at 45 °C, the h_{den} of untreated samples and samples containing 1 g/100 g NaCl
293 increased significantly in magnitude, indicating that peak 2 was partly covered by peak 1 during the
294 initial temperature range, and then grew as myosin was denatured. The same might be the case for
295 the sudden appearance of peak 2 after heating at 30 °C for samples containing 3 g/100 g NaCl. This
296 peak was not visible after heating at lower and higher temperatures. Actin seemed to be less heat-
297 stable for salted samples than for unsalted samples, as the h_{den} of peak 3 decreased in magnitude
298 after heating at 45 °C or higher for samples containing 1 g/100 g NaCl, but generally remained at a
299 larger magnitude for unsalted samples until after heating at 70 °C. After heating at 40 °C or higher, all
300 peaks had disappeared completely from the thermographs of samples containing 3 g/100 g NaCl. This
301 indicates that for this salt concentration, any changes in 3D-conformational structure of the muscle
302 proteins after 40 °C were either too gradual or did not involve sufficient energy dissipation to be
303 visualized in the DSC thermographs.

304 3.3. Water holding capacity

305 In Figure 4a, data for water holding capacity (WHC) of brined cod are shown with data for untreated
306 cod (Blikra *et al.*, 2019) as a function of heating temperature. As can be seen from the figure, salting
307 increased the WHC of the fish after heating at all tested temperatures. Samples containing 3 g/100 g

308 NaCl generally showed a higher WHC than the samples containing 1 g/100 g NaCl, although not
309 always significant. This is in agreement with a previous study, where WHC of cod increased with
310 increasing salt concentration in the brine added to ground cod, ranging from 0.3-1 g/100 g NaCl
311 (Johnsen *et al.*, 2009).

312 In Figure 4a, the water-brined samples showed a lower WHC compared to the untreated samples.
313 When considering the result in g hold water /g dry matter (Figure 4b), the results for untreated and
314 water-brined samples were almost identical, showing that the absorbed water during brining could
315 explain the difference in water holding capacity expressed as mass fraction of final to initial weight.
316 The result for water-brined cod (Figure 4a) was similar to data for post-rigor fileted cod (Skipnes *et*
317 *al.*, 2011), which is known to contain more water than pre-rigor fileted cod (Kristoffersen *et al.*,
318 2006a).

319 The experimental data was fitted to a function for the change in WHC with temperature (van der
320 Sman (2007); Eq. 8):

$$321 \quad C_{eq}(T) = C_{eq,0} - \frac{a_1}{1+a_2 \exp(-a_3(T-T_\sigma))} \quad (8)$$

322 where $C_{eq,0}$ is the initial WHC of raw sample, T is the temperature in °C, T_σ is the center of a logistic
323 curve, and a_1 , a_2 , and a_3 are fitting parameters determined by trial-and-error (Table 1). The
324 functions are shown in Figure 4a with the measured data. There was a general trend in all sample
325 groups of higher WHC for samples not previously heated and samples heated at 30 °C, followed by a
326 significant drop with a local minimum after isothermal heating treatments from 45-50 °C. For
327 unsalted samples and samples containing 1 g/100 g NaCl, this drop corresponded to denaturation of
328 peak 1, attributed to myosin.

329 It should be noted that while water-brined cod fit the sigmoidal curve type well, salted cod changed
330 in a different manner. In contrast to water-brined samples and samples containing 3 g/100 g NaCl,
331 the WHC of cod containing 1 g/100 g NaCl increased slightly after heating at 50-55 °C. The same
332 increase was also observed after heating at 40-50 °C for untreated cod (Blikra *et al.*, 2019). Since the

333 result was not significantly different from the results for samples treated at temperatures
334 immediately lower or higher than 50-55 °C (namely 40-65 °C), this rise was not included in the
335 parameters of Eq. 8. Cod containing 3 g/100 g NaCl showed a more gradual decrease in WHC with
336 increasing temperature than all other sample groups, and as a consequence, the sigmoidal type
337 equation could not capture all the measurement points. Rather, during the equation fitting we aimed
338 to obtain a good prediction for a maximum of temperatures. The equation should be validated
339 experimentally using the measured mass loss during heating. If substantial deviations are found
340 between measured and predicted results, fitting the data to a more complex equation type can be
341 considered.

342 3.4. Rheology

343 The storage modulus of cod samples with all salt concentrations tested followed the same overall
344 trend of lower initial values (0-50 °C), then a rapid rise (50-70 °C), and finally a plateau (80-100 °C;
345 Figure 5). The slope found between 50-75 °C was very similar for all sample groups. Significant
346 differences between the storage modulus of some of the sample groups were found in the
347 temperature range 0-40 °C, but none from 45-80 °C. However, there were some clear trends in the
348 average values. The initial storage modulus for unsalted cod was higher than for the salted samples,
349 which corresponds well with the decreased hardness of salted fish muscle compared to unsalted in
350 the literature (Esaiassen et al., 2004; Kong et al., 2008; Larsen et al., 2008). Cod containing 3 g/100 g
351 NaCl showed a different behavior than the other concentrations in that there was a local maximum
352 in storage modulus observed between 40-44 °C for all parallels (n=10). This peak resulted in a
353 significant difference in storage modulus between the samples containing 1 and 3 g/100 g NaCl at 40
354 °C. During DSC analysis of raw samples containing 3 g/100 g NaCl, a very low residual denaturation
355 enthalpy of peak 3 (actin) was visible at a PDT of around 67 °C (Figure 3). However, after isothermal
356 heat treatment at 40 °C for 10 min, this peak had disappeared, which indicates that actin easily
357 denatures even at 40 °C in cod samples of this salt concentration. Thus, the local maximum in G' at
358 40-44 °C observed for samples of 3 g/100 g NaCl could be attributed to hardening as a consequence

359 of denaturation of actin. For the same salt concentration, a significant reduction in WHC occurred
360 between isothermal heating temperatures of 35-40 °C (P=0.000; Figure 4). Since myosin was
361 denatured after isothermally heating at 35 °C, the reduction in WHC of samples of this salt
362 concentration could perhaps also be attributed to denaturation of actin. After reaching 50 °C, the G'
363 of samples containing 3 g/100 g NaCl increased steadily until reaching around 75 °C, like the other
364 samples, despite actin most probably already being denatured. The continued increase in G' could
365 result from protein aggregation, which has been reported for isolated myosin from cod
366 (Yongsawatdigul & Park, 1999), as well as for isolated myosin and myofibrils from white muscle of
367 salmon (Lefevre, Fauconneau, Thompson, & Gill, 2007).

368 The change in storage modulus (G') as a function of temperature was fitted to sigmoidal curves
369 (Figure 5; Eq. 9), as previously published for meat (Feyissa *et al.*, 2013), chicken breast (Rabeler &
370 Feyissa, 2018a) and unsalted cod (Blikra *et al.*, 2019). In Equation 9, G'_{max} and G'_{min} are the average
371 maximum and minimum storage moduli, respectively, T is the temperature (°C), and g_1 and g_2 are
372 fitting parameters determined by trial-and-error, supplied in Table 1.

$$373 \quad G'(T) = G'_{max} + \frac{G'_{min} - G'_{max}}{1 + \exp\left(\frac{T - g_1}{g_2}\right)} \quad (9)$$

374 3.5. Microstructure

375 Micrographs showing an average cross-sectional muscle structure for each sample parameter are
376 shown in Figure 6. Muscle bundles can be seen as orange structures surrounded by white channels.
377 The white channels can be regarded as areas where water can be transported during cooking without
378 disrupting the structure. There were no visible spaces present between the muscle bundles of
379 samples containing 3 g/100 g NaCl (Figure 6d), probably as a result of muscle structure swelling
380 during brining, which has also been reported by other authors (Ofstad *et al.*, 1996). The water-brined
381 samples (Figure 6b), on the other hand, showed a greater extent of widened channels than the other
382 parameters (Figure 6a, c-d). It can be speculated that the water absorbed by these samples during
383 brining was kept “free” in channels between the muscle structures. Since the water added did not

384 contain any solutes, less suspended particles per g extracellular water would be present in the water-
385 brined fish muscle than in the untreated, and thus a lower number of nucleation sites during freezing
386 (Burgaard, 2010). This could result in formation of fewer and larger ice crystals compared to the other
387 sample groups and cause partial freeze denaturation of water-brined samples, which may have
388 caused the partially disrupted structure observed in Figure 6b. The elevated PDT of myosin observed
389 for water-brined samples compared to untreated samples (Section 3.1) could perhaps also be related
390 to this phenomenon. Moreover, the addition of brine (Figure 6c, d) could have caused better and
391 quicker freezing conditions due to the addition of solutes and thus nucleation sites in addition to
392 swelling. Therefore, it may be possible that the differences in microstructure not only reflect the
393 differences between salt concentrations directly, but also reflect the effect that these salt
394 concentrations have on protection of the muscle structure during this particular freezing regime
395 (Figure 1; Wolfe & Bryant, 2001).

396 3.6. Model prediction

397 The model prediction showed that salting reduced the predicted mass loss in a concentration
398 dependent manner (Figure 7). This was in accordance with the expected result, since it is known that
399 brining in low salt concentrations decrease the amount of liquid loss during cooking (eg. Kong *et al.*,
400 2008; Ofstad *et al.*, 1996).

401 For water-brined samples, less water loss was predicted than for untreated fish (Figure 10). Based on
402 first-hand experience, however, we know that the water-brined samples lose more water upon
403 cooking than untreated samples. Storage modulus and WHC were the major variables measured in
404 this study; however, the permeability of the muscle also affects the modeled result (Blikra, *et al.*,
405 2019). In the simulations performed in this study, the permeability was assumed to be constant, and
406 therefore a fixed value was used for all sample parameters. However, since larger gaps were seen
407 between the muscle cells of water-brined samples than untreated samples (Figure 9) it is expected
408 that the permeability, in which pore size is a contributing factor (Datta, 2006), will be higher for the
409 former group, which would increase the predicted mass loss.

410 4. Conclusion

411 In this study, quality parameters of brined cod were investigated and used in a physics-based model
412 to estimate water retention during heating. Equations describing the temperature dependency of the
413 storage modulus and water holding capacity (WHC) for water-brined samples (0.06 g/100 g NaCl) and
414 salted samples containing 1 and 3 g/100 g NaCl were developed. Samples containing 3 g/100 g NaCl
415 showed significantly higher WHC than unsalted cod. Salting also showed a profound effect on the
416 denaturation enthalpy and peak denaturation temperature of the three visible protein denaturation
417 peaks. Salting lowered the denaturation temperature and reduced the magnitude of the observed
418 residual enthalpy of the peaks attributed to myosin and actin. Considering the peak attributed to
419 sarcoplasmic proteins, no difference was observed between untreated samples and samples
420 containing 1 g/100 g NaCl. This peak was, however, camouflaged or denatured after heating at all
421 tested temperatures except 30 °C for samples containing 3 g/100 g NaCl.

422 Mathematical modeling was used to investigate how the functions for storage modulus and WHC
423 affected the predicted change in water content of cod during heating. The model prediction showed
424 that cod containing 1-3 g/100 g NaCl had a higher water retention compared to unsalted samples,
425 which was in agreement with experimental data obtained in other studies (Kong *et al.*, 2008; Ofstad
426 *et al.*, 1996).

427 The model predictions remain to be quantitatively validated in later studies. This validation may be
428 combined with an optimization study of a commercial product to prove the industrial impact of this
429 innovative model. In addition, accurate values for the permeability of cod muscle is needed to
430 acquire more accurate model solutions.

431 Acknowledgements

432 This work was supported by the Norconserv Foundation, the Research Council of Norway, and the
433 Technical University of Denmark (DTU). We would like to thank Vanessa Meling, Hrant Shamiran and

434 Ida Bjørnstad for their Bachelor thesis work at the University of Stavanger under our supervision at
435 Nofima.

436 References

437 Asaria, P., Chisholm, D., Mathers, C., Ezzati, M., & Beaglehole, R. (2007). Chronic disease prevention:
438 Health effects and financial costs of strategies to reduce salt intake and control tobacco use.
439 *The Lancet*, 370, 2044-2053.

440 Barrière, B., & Leibler, L. (2003). Kinetics of solvent absorption and permeation through a highly
441 swellable elastomeric network. *Journal of Polymer Science Part B: Polymer Physics*, 41, 166-
442 182.

443 Bearth, A., Cousin, M.-E., & Siegrist, M. (2014). The consumer's perception of artificial food additives:
444 Influences on acceptance, risk and benefit perceptions. *Food Quality and Preference*, 38, 14-
445 23.

446 Blikra, M. J., Skipnes, D., & Feyissa, A. H. (2019). Model for heat and mass transport during cooking of
447 cod loin in a convection oven. *Food Control*, 102, 29-37.

448 Burgaard, M. G. (2010). Effect of frozen storage temperature on quality-related changes in fish
449 muscle: Changes in physical, chemical and biochemical quality indicators during short- and
450 long-term storage [PhD thesis]. Søborg: DTU Food.

451 Burgaard, M. G., & Jørgensen, B. M. (2010). Effect of temperature on quality-related changes in cod
452 (*Gadus morhua*) during short- and long-term frozen storage. *Journal of Aquatic Food Product*
453 *Technology*, 19, 249-263.

454 Cheow, C. S., Yu, S. Y., & Howell, N. K. (1999). Effect of salt, sugar and monosodium glutamate on the
455 viscoelastic properties of fish cracker ("Keropok") gel. *Journal of Food Processing and*
456 *Preservation*, 23, 21-37.

457 Datta, A. K. (2006). Hydraulic permeability of food tissues. *International Journal of Food Properties*, 9,
458 767-780.

459 Datta, A. K. (2007). Porous media approaches to studying simultaneous heat and mass transfer in
460 food processes. I: Problem formulations. *Journal of Food Engineering*, 80, 80-95.

461 Esaiassen, M., Østli, J., Elvevoll, E. O., Joensen, S., Prytz, K., & Richardsen, R. (2004). Brining of cod
462 fillets: Influence on sensory properties and consumers liking. *Food Quality and Preference*,
463 15, 421-428.

464 Evans, G., de Challemaison, B., & Cox, D. N. (2010). Consumers' ratings of the natural and unnatural
465 qualities of foods. *Appetite*, 54, 557-563.

466 Feyissa, A. H., Gernaey, K. V., & Adler-Nissen, J. (2013). 3D modelling of coupled mass and heat
467 transfer of a convection-oven roasting process. *Meat Science*, 93, 810-820.

468 Hastings, R. J., Rodger, G. W., Park, R., Matthews, A. D., & Anderson, E. M. (1985). Differential
469 scanning calorimetry of fish muscle: The effect of processing and species variation. *Journal of*
470 *Food Science*, 50, 503-506.

471 He, F. J., & MacGregor, G. A. (2009). A comprehensive review on salt and health and current
472 experience of worldwide salt reduction programmes. *Journal of Human Hypertension*, 23,
473 363-384.

474 Hultmann, L., Tobiassen, T., Aas-Hansen, Ø., Phu, T. M., & Rustad, T. (2016). Muscle quality and
475 proteolytic enzymes of farmed Atlantic cod (*Gadus morhua*) during storage: Effects of pre-
476 slaughter handling and increased storage temperature. *Journal of Aquatic Food Product*
477 *Technology*, 25, 540-554.

478 Johnsen, S. O., Jørgensen, K. B., Birkeland, S., Skipnes, D., & Skåra, T. (2009). Effects of phosphates
479 and salt in ground raw and cooked farmed cod (*Gadus morhua*) muscle studied by the water
480 holding capacity (WHC), and supported by ³¹P-NMR measurements. *Journal of Food Science*,
481 74, C211-C220.

482 Kobayashi, Y., & Park, J. W. (2017). Physicochemical characterizations of tilapia fish protein isolate
483 under two distinctively different comminution conditions. *Journal of Food Processing and*
484 *Preservation*, 41, E13233.

485 Kong, F., Oliveira, A., Tang, J., Rasco, B., & Crapo, C. (2008). Salt effect on heat-induced physical and
486 chemical changes of salmon fillet (*O. gorbuscha*). *Food chemistry*, *106*, 957-966.

487 Kong, F., Tang, J., Rasco, B., & Crapo, C. (2007). Kinetics of salmon quality changes during thermal
488 processing. *Journal of Food Engineering*, *83*, 510-520.

489 Kristoffersen, S., Tobiassen, T., Esaiassen, M., Olsson, G. B., Godvik, L. A., Seppola, M. A., & Olsen, R.
490 L. (2006a). Effects of pre-rigour filleting on quality aspects of Atlantic cod (*Gadus morhua* L.).
491 *Aquaculture Research*, *37*, 1556-1564.

492 Kristoffersen, S., Tobiassen, T., Steinsund, V., & Olsen, R. L. (2006b). Slaughter stress, postmortem
493 muscle pH and rigor development in farmed Atlantic cod (*Gadus morhua* L.). *International*
494 *Journal of Food Science and Technology*, *41*, 861-864.

495 Kristoffersen, S., Vang, B., Larsen, R., & Olsen, R. L. (2007). Pre-rigour filleting and drip loss from fillets
496 of farmed Atlantic cod (*Gadus morhua* L.). *Aquaculture Research*, *38*, 1721-1731.

497 Lambert, Y., & Dutil, J.-D. (1997). Can simple condition indices be used to monitor and quantify
498 seasonal changes in the energy reserves of Atlantic cod (*Gadus morhua*)? *Canadian Journal*
499 *of Fisheries and Aquatic Sciences*, *54*, 104-112.

500 Larsen, R., & Elvevoll, E. O. (2008). Water uptake, drip losses and retention of free amino acids and
501 minerals in cod (*Gadus morhua*) fillet immersed in NaCl or KCl. *Food Chemistry*, *107*, 369-376.

502 Larsen, R., Olsen, S. H., Kristoffersen, S., & Elvevoll, E. O. (2008). Low salt brining of pre-rigour filleted
503 farmed cod (*Gadus morhua* L.) and the effects on different quality parameters. *LWT-Food*
504 *Science and Technology*, *41*, 1167-1172.

505 Lefevre, F., Fauconneau, B., Thompson, J. W., & Gill, T. A. (2007). Thermal denaturation and
506 aggregation properties of Atlantic salmon myofibrils and myosin from white and red muscles.
507 *Journal of Agricultural and Food Chemistry*, *55*, 4761-4770.

508 NMKL 184 (2006). Aerobic count and specific spoilage organisms in fish and fish products.

509 Ofstad, R., Kidman, S., Myklebust, R., Olsen, R. L., & Hermansson, A.-M. (1996). Factors influencing
510 liquid-holding capacity and structural changes during heating of comminuted cod (*Gadus*
511 *morhua* L.) muscle. *LWT-Food Science and Technology*, *29*, 173-183.

512 Ovissipour, M., Rasco, B., Tang, J., & Sablani, S. (2017). Kinetics of protein degradation and physical
513 changes in thermally processed Atlantic salmon (*Salmo salar*). *Food and Bioprocess*
514 *Technology*, *10*, 1865-1882.

515 Rabeler, F., & Feyissa, A. H. (2018a). Kinetic modeling of texture and color changes during thermal
516 treatment of chicken breast meat. *Food and Bioprocess Technology*, *11*, 1495-1504.

517 Rabeler, F., & Feyissa, A. H. (2018b). Modelling the transport phenomena and texture changes of
518 chicken breast meat during the roasting in a convective oven. *Journal of Food Engineering*,
519 *237*, 60-68.

520 Singh, R. P., & Heldman, D. R. (2014). Appendix A.4 Physical properties of water and air. In S. L. Taylor
521 (Ed.), *Introduction to Food Engineering* (5th ed.). London, England: Elsevier, Academic Press.

522 Skipnes, D., Johnsen, S. O., Skåra, T., Sivertsvik, M., & Lekang, O. (2011). Optimization of heat
523 processing of farmed Atlantic cod (*Gadus morhua*) muscle with respect to cook loss, water
524 holding capacity, color, and texture. *Journal of Aquatic Food Product Technology*, *20*, 331-
525 340.

526 Skipnes, D., Østby, M. L., & Hendrickx, M. E. (2007). A method for characterising cook loss and water
527 holding capacity in heat treated cod (*Gadus morhua*) muscle. *Journal of Food Engineering*,
528 *80*, 1078-1085.

529 Skipnes, D., Van der Plancken, I., Van Loey, A., & Hendrickx, M. E. (2008). Kinetics of heat
530 denaturation of proteins from farmed Atlantic cod (*Gadus morhua*). *Journal of Food*
531 *Engineering*, *85*, 51-58.

532 Thorarinsdottir, K. A., Arason, S., Geirsdottir, M., Bogason, S. G., & Kristbergsson, K. (2002). Changes
533 in myofibrillar proteins during processing of salted cod (*Gadus morhua*) as determined by
534 electrophoresis and differential scanning calorimetry. *Food Chemistry*, *77*, 377-385.

- 535 Valle, F. R. D., & Nickerson, J. T. R. (1968). Salting and drying fish. 3. Diffusion of water. *Journal of*
536 *Food Science*, 33, 499-503.
- 537 van der Sman, R. G. M. (2007). Soft condensed matter perspective on moisture transport in cooking
538 meat. *American Institute of Chemical Engineers*, 53, 2986-2995.
- 539 Wolfe, J., & Bryant, G. (2001). Cellular cryobiology: Thermodynamic and mechanical effects.
540 *International Journal of Refrigeration*, 24, 438-450.
- 541 Yongsawatdigul, J., & Park, J. (1999). Thermal aggregation and dynamic rheological properties of
542 Pacific whiting and cod myosins as affected by heating rate. *Journal of Food Science*, 64, 679-
543 683.
- 544 Zink, D. L. (1997). The impact of consumer demands and trends on food processing. *Emerging*
545 *Infectious Diseases*, 3, 467-469.

Table 1. Fish characterization and model parameters.

		g/100 g NaCl in brine			
Property		Untreated	0	1.5	4.5
Characterization	Weight gain during brining (g 100/g initial weight, n=10)	–	8±3 ^a	11±1 ^a	24±5 ^b
	Final muscle pH (n=10)	6.22±0.08 ^{ab}	6.27±0.06 ^a	6.23±0.02 ^{ab}	6.10±0.06 ^b
	NaCl content (g/100 g, n=8)	0.10±0.02 ^a	0.06±0.03 ^a	1.00±0.17 ^b	3.06±0.58 ^c
	Moisture content (g/100 g, n=8)	77.3±0.4 ^a	80.1±1.1 ^b	80.6±1.9 ^b	80.2±2.2 ^b
Eq. 8. WHC	$C_{eq,0}$	0.82*	0.70	0.85	0.98
	a_1	0.12*	0.13	0.17	0.32
	a_2	23*	23	25	20
	a_3	0.42*	0.35	0.42	0.08
	T_σ	25*	30	32	16
Eq 9. G`	G'_{max} (kPa)	48±9*	38±9	42±7	38±8
	G'_{min} (kPa)	14±3*	13±5	10±2	15±1
	g_1	64*	64	60	63
	g_2	5*	4	7	5

Values in a row not sharing a common letter are significantly different ($P < 0.05$).

*Data published by Blikra *et al.* (2019).

Figure 1. **Flow chart of processing and sample preparation steps.**

Figure 2. **Normalized examples of DSC thermographs for raw samples of all salt concentrations heated at 2.5 K/min from 2-100 °C.**

Figure 3. **Residual denaturation enthalpy (h_{den}) and peak denaturation temperature (PDT) of heated cod muscle of various salt concentrations.** Peaks 1 (A-B), 2 (C-D) and 3 (E-F) are shown for raw samples and samples isothermally heated for 10 minutes at 25-65 °C, \pm SD (n=2). Cross: Untreated; Triangle: Water-brined; Diamond: 1 g/100 g NaCl; and Line: 3 g/100 g NaCl.

Figure 4. **Water holding capacity of raw and heat-treated cod muscle of various salt concentrations (\pm SD).** A) measurements (symbols) and equations (lines) in w/w percentage of raw sample weight; and B) measurements in g hold water /g dry water. Cross: Untreated; Yellow triangle: Water-brined; Orange diamonds: 1 g/100 g NaCl; and red circles: 3 g/100 g NaCl.

Figure 5. **Storage modulus of cod muscle of various salt concentrations.** A) Untreated; B) Water-brined; C) 1 g/100 g NaCl; D) 3 g/100 g NaCl. The dashed lines show measurements (n=10), and the solid lines show the corresponding equation. For clarity, SD is shown every 10 °C.

Figure 6. **Cross-sectional representative images of the microstructure of cod muscle of various salt concentrations (n=3).** A) Untreated; B) Water-brined; C) 1 g/100 g and d) 3 g/100 g NaCl.

Figure 7. **Model prediction of water retention in samples of cod muscle containing various salt concentrations.** Black: Untreated; Yellow: Water-brined; Orange: 1 g/100 g NaCl; and Red: 3 g/100 g NaCl.

Figure

[Click here to download high resolution image](#)

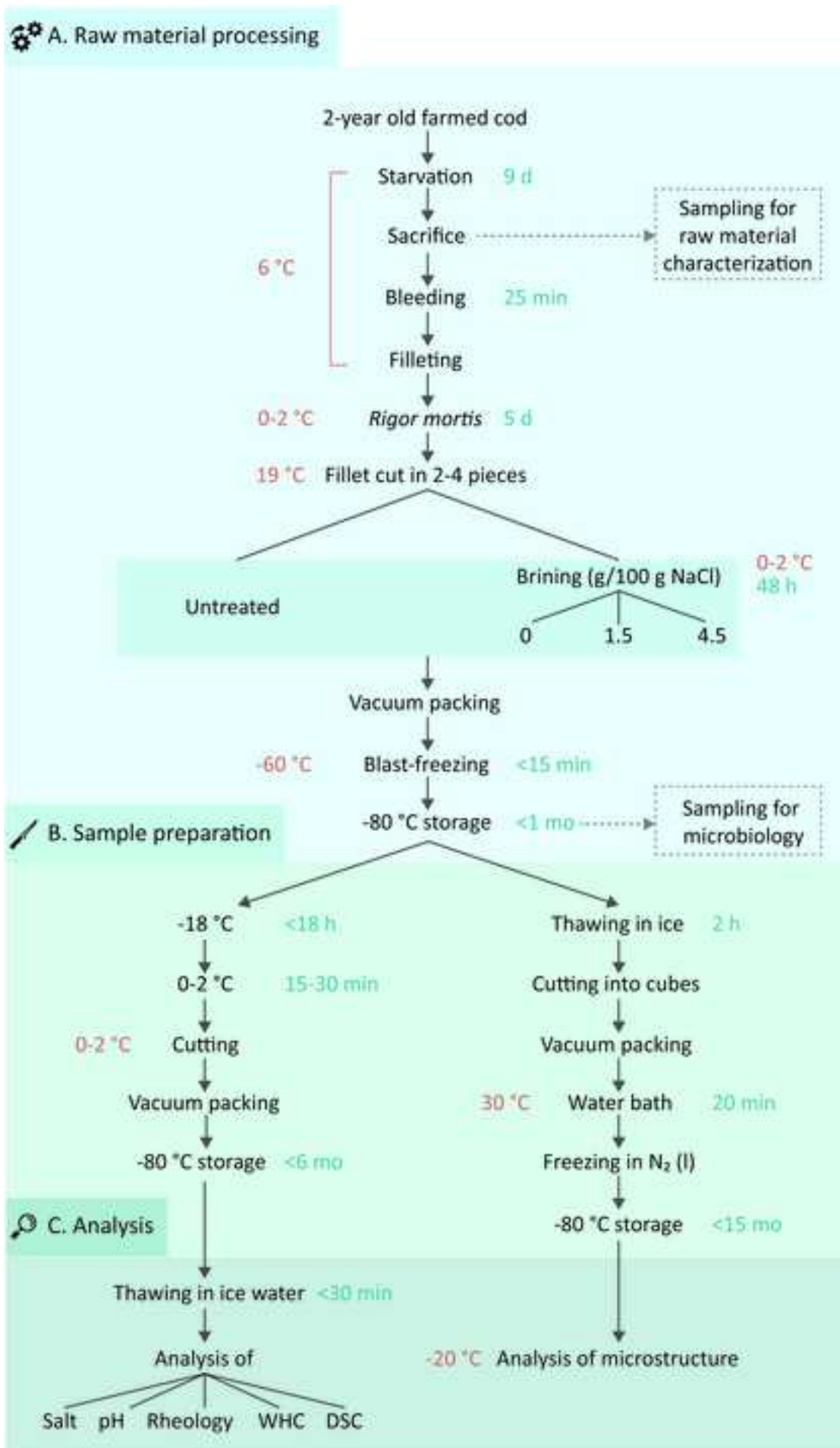
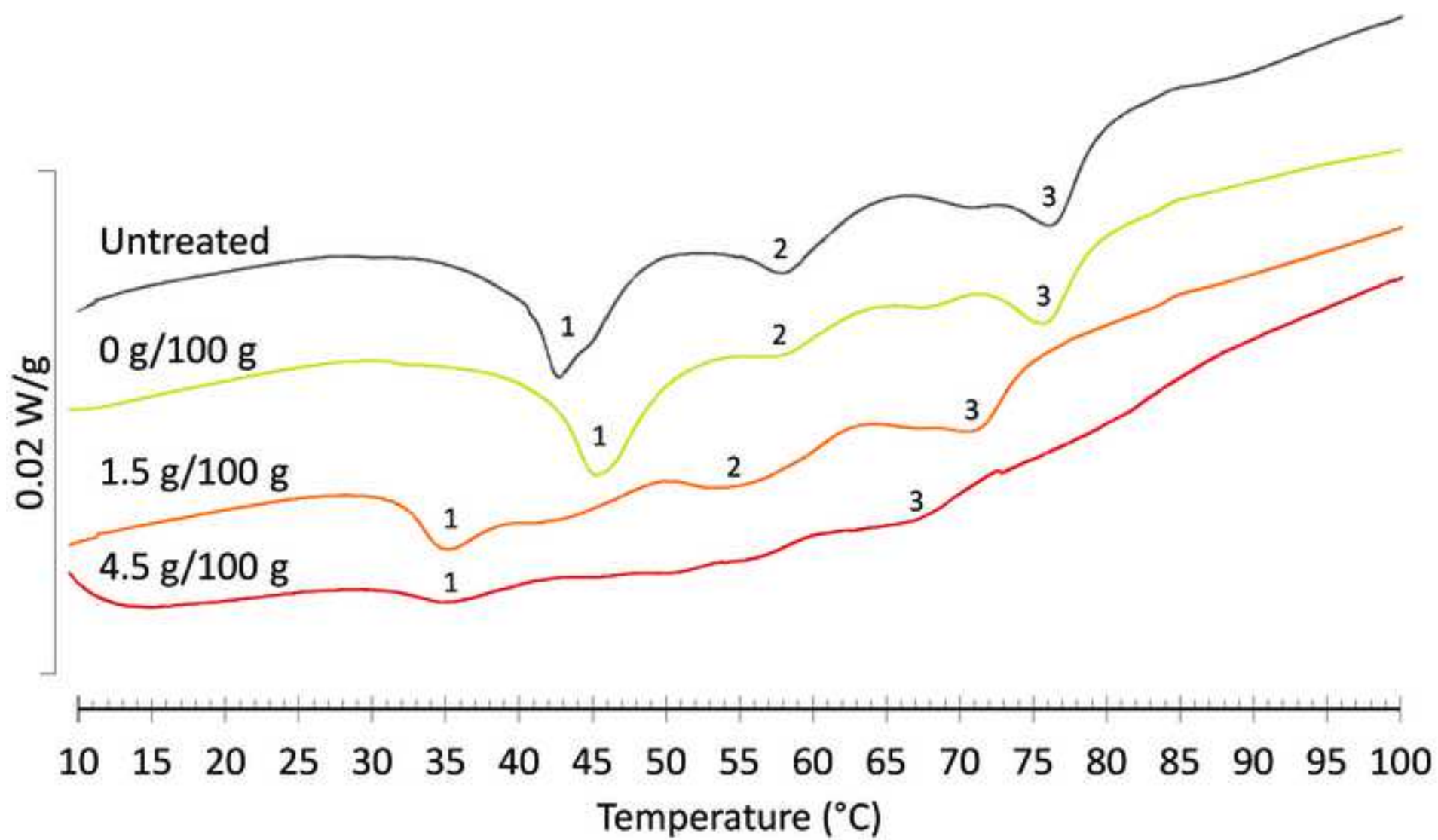


Figure
[Click here to download high resolution image](#)



Figure

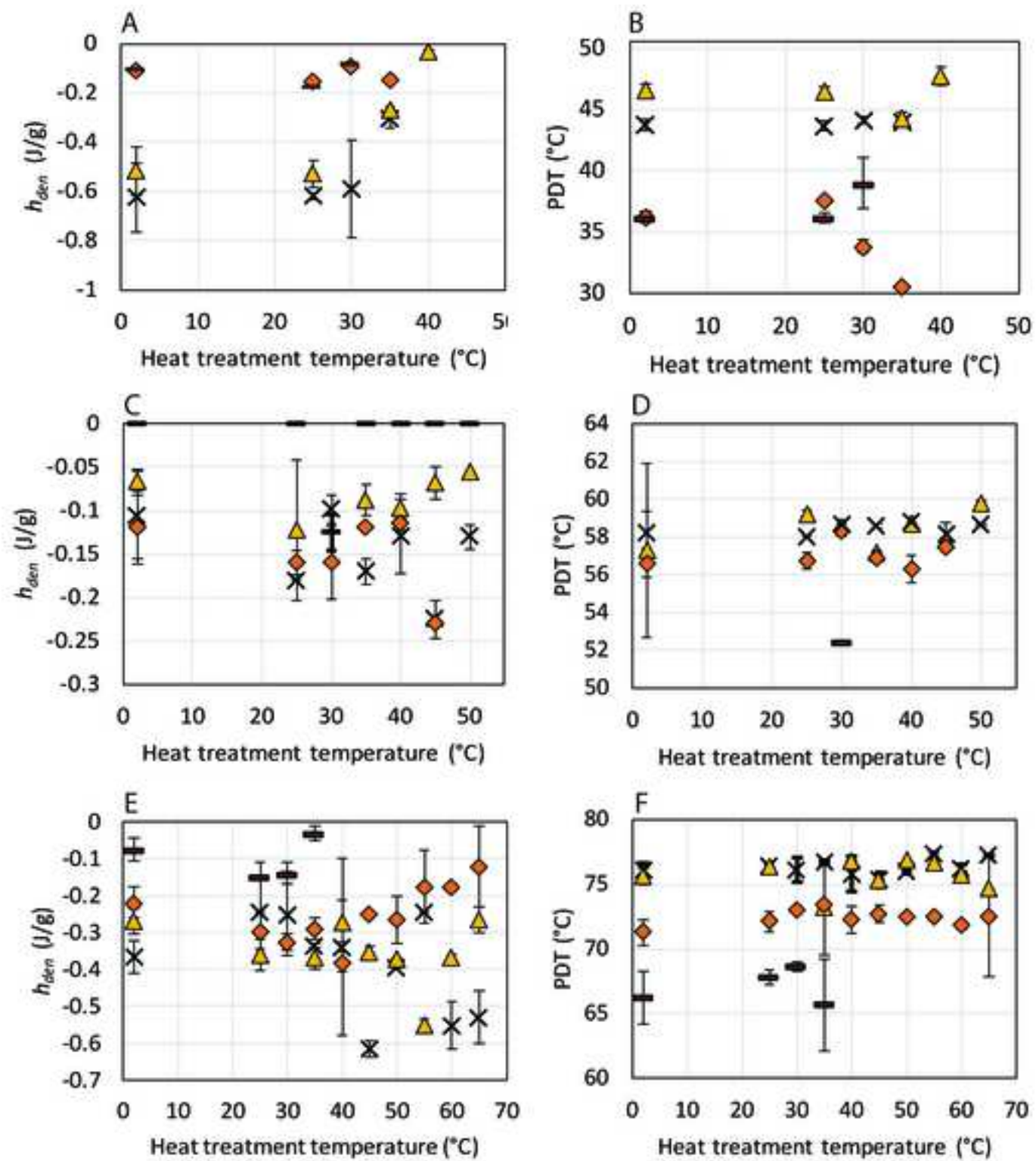
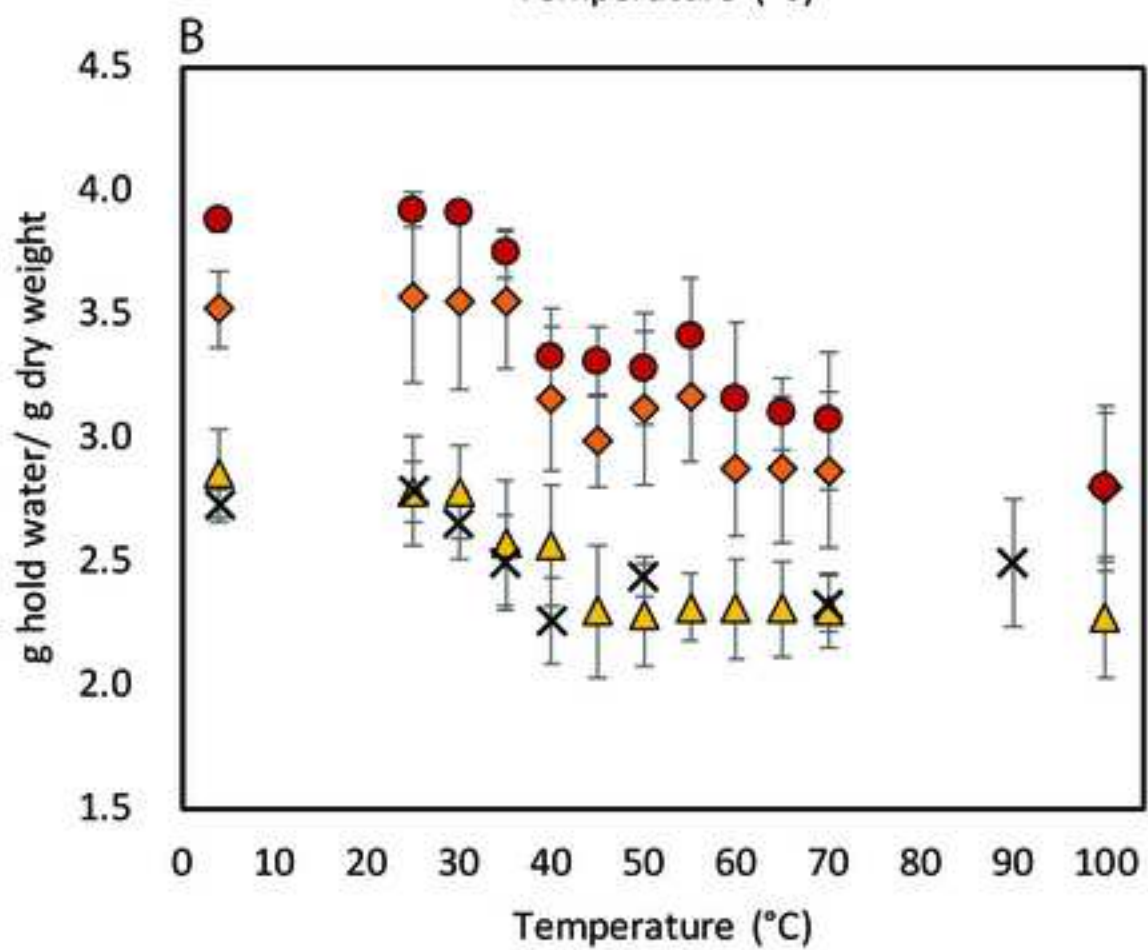
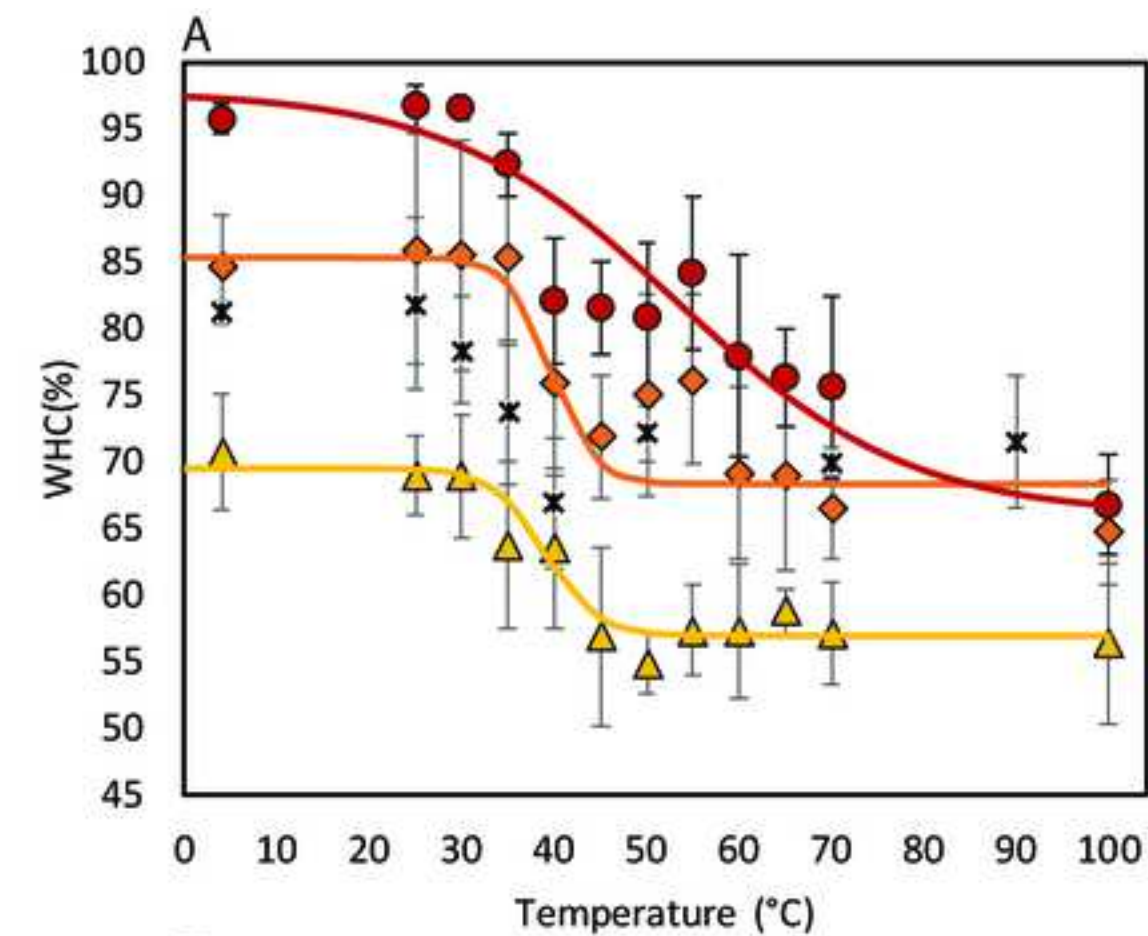
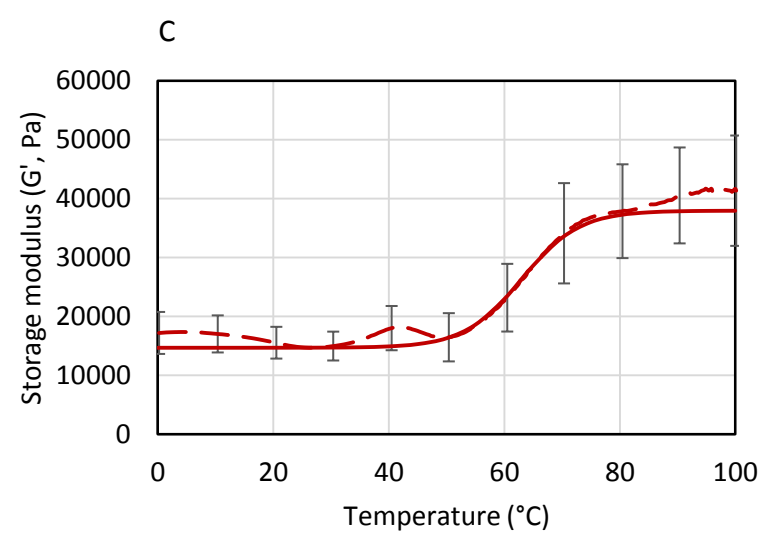
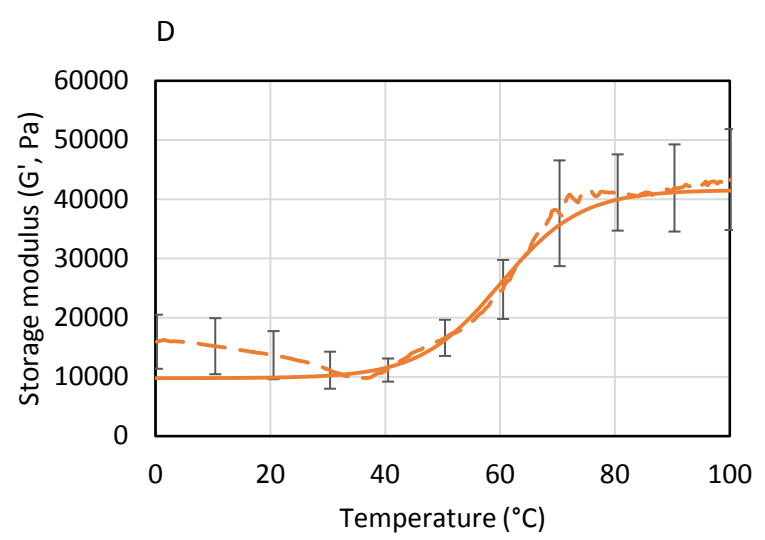
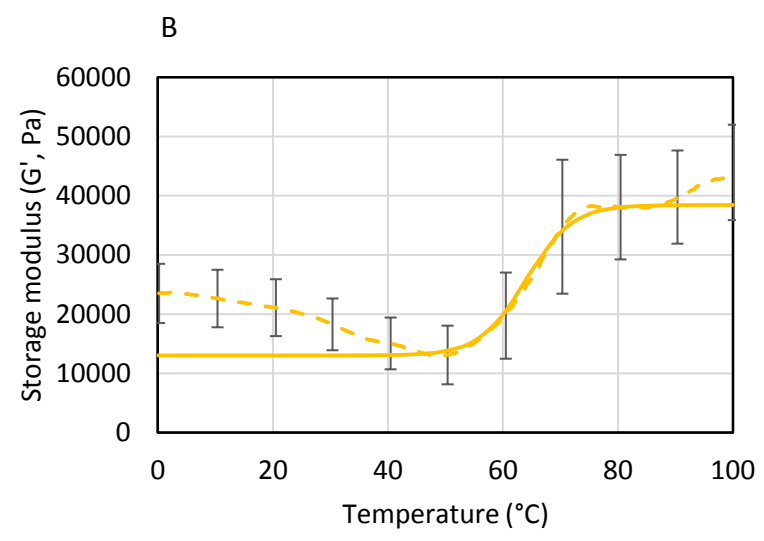
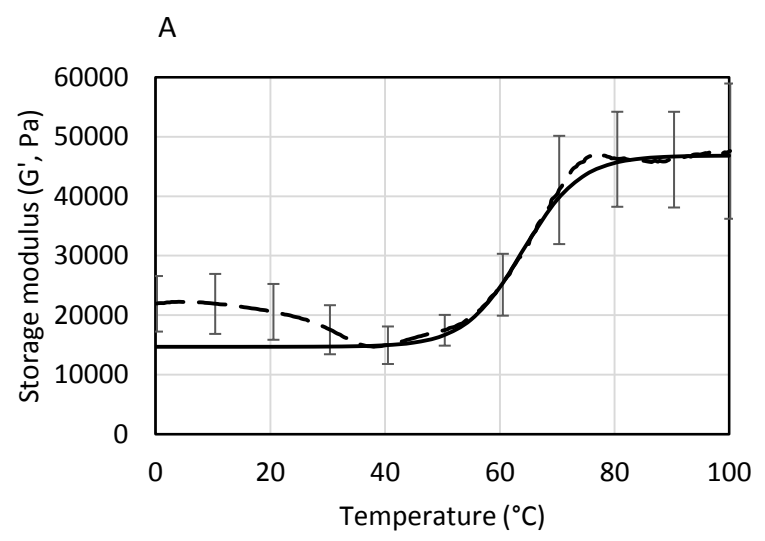
[Click here to download high resolution image](#)

Figure
[Click here to download high resolution image](#)



Figure



Figure

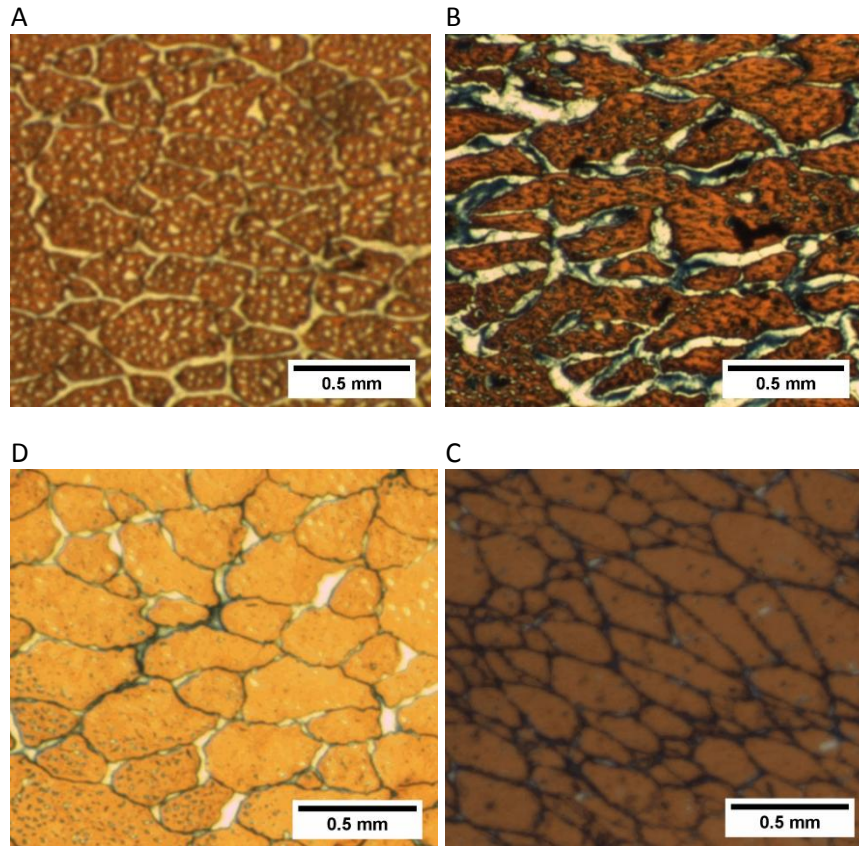


Figure
[Click here to download high resolution image](#)

